Published in final edited form as:
J Immunol. 2009 December 1; 183(11): 7411–7419. doi:10.4049/jimmunol.0804343.

Increased Inflammation, Impaired Bacterial Clearance, and Metabolic Disruption after Gram-Negative Sepsis in *Mkp-1*-Deficient Mice[1]

W. Joshua Frazier[*,†], **Xianxi Wang**[*], **Lyn M. Wancket**[‡], **Xiang-An Li**[§], **Xiaomei Meng**[*], **Leif D. Nelin**[*,†], **Andrew C. B. Cato**[¶], and **Yusen Liu**[*,†,‡,2]

[*] Center for Perinatal Research, The Research Institute at Nationwide Children's Hospital, Columbus, OH 43205

[†] Department of Pediatrics, The Ohio State University College of Medicine, Columbus, OH 43210

[‡] Department of Veterinary Biosciences, The Ohio State University College of Veterinary Medicine, Columbus, OH 43210

[§] Department of Pediatrics, University of Kentucky Medical School, Lexington, KY 40536

[¶] Forschungszentrum Karlsruhe, Institute of Toxicology and Genetics, Karlsruhe, Germany

Abstract

MAPKs are crucial for TNF-α and IL-6 production by innate immune cells in response to TLR ligands. MAPK phosphatase 1 (Mkp-1) deactivates p38 and JNK, abrogating the inflammatory response. We have previously demonstrated that *Mkp-1*$^{-/-}$ mice exhibit exacerbated inflammatory cytokine production and increased mortality in response to challenge with LPS and heat-killed *Staphylococcus aureus.* However, the function of Mkp-1 in host defense during live Gram-negative bacterial infection remains unclear. We challenged *Mkp-1*$^{+/+}$ and *Mkp-1*$^{-/-}$ mice with live *Escherichia coli* i.v. to examine the effects of *Mkp-1* deficiency on animal survival, bacterial clearance, metabolic activity, and cytokine production. We found that Mkp-1 deficiency predisposed animals to accelerated mortality and was associated with more robust production of TNF-α, IL-6 and IL-10, greater bacterial burden, altered cyclooxygenase-2 and iNOS expression, and substantial changes in the mobilization of energy stores. Likewise, knockout of *Mkp-1* also sensitized mice to sepsis caused by cecal ligation and puncture. IL-10 inhibition by neutralizing Ab or genetic deletion alleviated increased bacterial burden. Treatment with the bactericidal antibiotic gentamicin, given 3 h after *Escherichia coli* infection, protected *Mkp-1*$^{+/+}$ mice from septic shock but had no effect on *Mkp-1*$^{-/-}$ mice. Thus, during Gram-negative bacterial sepsis Mkp-1 not only plays a critical role in the regulation of cytokine production but also orchestrates the bactericidal activities of the innate immune system and controls the metabolic response to stress.

Severe sepsis and septic shock, the most dire manifestations of bacterial infection in humans, are major contributors to morbidity and mortality worldwide. Mortality from septic shock in adult patients approaches 50%, with survivors often facing serious disabilities (1,2). Excessive production of inflammatory cytokines with resultant vascular collapse has been implicated in

[1]This work was supported by the National Institutes of Health Grants AI68956 and AI57798 (to Y.L.).

[2]Address correspondence and reprint requests to Dr. Yusen Liu, Center for Perinatal Research, The Research Institute at Nationwide Children's Hospital, 700 Children's Drive, Columbus, OH 43205. yusen.liu@nationwidechildrens.org.

Disclosures
The authors have no financial conflict of interest.

early mortality from septic shock and contributes to the development of multiorgan dysfunction syndrome (3). Dysregulation of innate immune responses has been implicated in a variety of human inflammatory diseases, including septic shock (4–6). During microbial infection, innate immune effector cells (e.g., mononuclear monocytes/macrophages) recognize pathogens through highly conserved, constitutively expressed pattern recognition receptors. Interaction of these pattern recognition receptors, such as TLRs, with microbe-associated molecular patterns activates a variety of signal transduction pathways, leading to the production of inflammatory cytokines and initiation of downstream inflammatory cascades (6–11). Among the critical pathways mediating the inflammatory response is the MAPK system, including ERK, JNK, and p38 (8,12,13). These MAPKs regulate immune responses at multiple levels, including facilitation of Ag presentation and induction of cytokine expression (12). Inflammatory cytokines in turn mediate a number of physiologic changes characteristic of the inflammatory response, including recruitment and activation of monocytes and other phagocytes (7). In addition to influencing the local inflammatory milieu in the host, proinflammatory cytokines affect a variety of changes in organs and tissues remote from the site of infection, such as alterations in body temperature, capillary permeability, and activation of the adaptive immune system (3,8,9,14). In addition to releasing cytokines to alter host physiology in response to infection, innate immune cells are responsible for the earliest phases of fending off infection through the killing and processing of microbes. Monocytes/macrophages engulf pathogens by phagocytosis. Intracellular killing of bacteria is accomplished through the generation of reactive oxygen and nitrogen species within the phagolysosome by enzymes such as myeloperoxidase (MPO)[3] and inducible NO synthase (iNOS), which in turn lyse bacterial cell walls (15,16). Pathogen-derived antigenic peptides are then presented by the monocyte/macrophage to elements of the adaptive immune system (7).

Inflammatory insults often cause a shift to catabolic pathways and mobilization of energy stores (17,18). Catabolism is characterized by protein breakdown in the liver and skeletal muscle, increased glycogenolysis, and enhanced lipolysis to release free fatty acids and triglycerides (18). Recent studies suggest that catabolic shifting both provides substrate for ongoing cellular metabolic processes and modulates host defense against invading pathogens (19,20). Each of these responses is crucial for host survival during infection. Additionally, although the inflammatory response is essential for preventing life-threatening infection, excessive or unregulated inflammation produces pathologic systemic derangements with vascular compromise and widespread collateral damage (3,8).

Previously, we and other investigators have shown that MAPK phosphatase 1 (Mkp-1) plays a pivotal role in regulation of the innate immune response (21–26). Mkp-1 protein inhibits proinflammatory cytokine production by dephosphorylating and thereby inactivating JNK and p38 after exposure to microbial products, such as the Gram-negative bacterial cell wall component LPS. In the absence of a functional *Mkp-1* gene, mice produce substantially greater quantities of inflammatory cytokines and exhibit increased mortality from endotoxic shock (23). Although the role of Mkp-1 in regulating the immune response to purified bacterial components has been well characterized, its role in the host response to live Gram-negative bacteria has not been described. Since live bacteria contain multiple antigenic components and can actively proliferate in the host, Mkp-1 may have additional novel functions in the regulation of the immune response and metabolism during live bacterial infection.

To understand the role of Mkp-1 in host defense against Gram-negative bacterial infection, we studied the immune and metabolic responses of *Mkp-1*$^{-/-}$ and *Mkp-1*$^{+/+}$ mice to both i.v. live

[3]Abbreviations used in this paper: MPO, myeloperoxidase; iNOS, inducible NO synthase; CLP, cecal ligation and puncture; COX-2, cyclooxygenase-2; Mkp-1, MAPK phosphatase 1.

Escherichia coli and mixed bacteria via cecal ligation and puncture (CLP). We found that Mkp-1 regulated cytokine production and was key to both bacterial killing and resource mobilization during Gram-negative bacterial infection. In addition, we demonstrated that antimicrobial therapy for Gram-negative sepsis was only effective in *Mkp-1*$^{+/+}$ mice, illustrating the critical role of Mkp-1 in determining the clinical outcome of such therapy.

Materials and Methods

Experimental animals

Mkp-1$^{-/-}$ mice have been described previously (27) and have no obvious phenotype before experimental use (22,27). *Mkp-1*$^{-/-}$ and *Mkp-1*$^{+/+}$ mice were provided by Bristol-Myers Squibb Pharmaceutical Research Institute and littermates on a C57/129 mixed background were used for all experiments except for studies specified using *Mkp-1*$^{-/-}$/*Il-10*$^{-/-}$ double knockout mice. For those studies, *Il-10*$^{-/-}$ mice (28) on a pure 129 background were obtained from The Jackson Laboratory. These mice were crossbred to *Mkp-1*$^{-/-}$ mice on a 129 background to yield *Mkp-1*$^{-/-}$/*Il-10*$^{-/-}$ double knockout mice. All mice were housed with a 12-h alternating light-dark cycle at 25°C, with humidity between 30% and 70% and free access to food and water. All experiments were performed according to National Institutes of Health guidelines and were approved by the Institutional Animal Care and Use Committee at the Research Institute at Nationwide Children's Hospital.

E. coli infection

A wild-type (smooth) strain of *E. coli* (O55:B5, ATCC 12014) was used for all experiments. This *E. coli* strain was the source of LPS used in previous studies in our laboratory (22,23). Bacteria were grown in Luria broth for 18 h at 37°C and bacterial CFU of each culture was determined by comparing the specific OD_{600} value to a standard curve. Bacteria were washed twice with sterile PBS and adjusted to the appropriate final concentration. For bacterial injection, mice were placed in a clear plastic restraining device and tails cleaned with 70% ethanol. The bacterial suspension was injected into the tail vein using a new syringe and needle for each mouse; the dose was 2.5×10^7 CFU/g of body weight unless otherwise specified. To avoid bias, *Mkp-1*$^{+/+}$ and *Mkp-1*$^{-/-}$ mice were injected in a blinded fashion.

Cecal ligation and puncture

CLP was performed as previously described (29). In brief, 8- to 12-wk-old *Mkp-1*$^{-/-}$ and *Mkp-1*$^{+/+}$ mice (n = 15/group) were anesthetized using 2–5% isoflurane in 100% oxygen. A midline incision (1.0 cm) was made below the diaphragm. The cecum was isolated, ligated, punctured twice with a 23-gauge needle, and then gently compressed to extrude a small amount of cecal contents. The cecum was returned to the abdomen and the muscle and skin incisions were closed with 6–0 Ethilon suture material. Mice received 1 ml of PBS subcutaneously after surgery and survival was monitored for 5 days.

Survival

Male *Mkp-1*$^{-/-}$ and *Mkp-1*$^{+/+}$ mice (8- to 12-weeks old; n = 10/group) were infected i.v. with live *E. coli*. Mice were observed every 3 to 4 h for death or moribund state through 72 h. Moribund animals and all mice alive at the end of the experiment were euthanized by CO_2 inhalation. To examine the effect of gentamicin on survival, mice were injected with *E. coli* i.v. and received a 25 μg/mouse dose of gentamicin sulfate (Sigma-Aldrich) subcutaneously 3 h postinfection. The gentamicin dose is comparable to doses used clinically to treat Gram-negative bacterial infections in humans (10 mg/kg/day). Gentamicin was administered in 1 ml of PBS, providing fluid support similar to treatment levels for sepsis in humans (nearly 40 ml/kg) (30–32).

Histological and biochemical analyses

Animals were weighed and euthanized 18 h or 24 h after *E. coli* infection by overdose of pentobarbital i.p. Blood was collected by cardiac puncture for a complete blood biochemical report (clinical laboratory at The Veterinary Hospital of The Ohio State University). Lungs, spleens, thymuses, and livers were harvested aseptically. The right lung was weighed and used to calculate lung weight/body weight ratio. The left lung was inflated, fixed in formalin, and routinely processed to produce H&E-stained sections for histological analysis. Livers and the right lung were snap frozen in liquid N_2 and stored at −80°C until analysis.

The MPO activity in frozen lungs was assessed as previously described (21). To evaluate the expression levels of iNOS and cyclooxygenase 2 (COX-2), frozen lung and liver tissues were homogenized and sonicated in a lysis buffer containing proteinase inhibitors. Triton X-100 was added to the homogenates to a final concentration of 1%, and the homogenates were incubated on ice for 15 min. After centrifugation at 14,000 × *g* for 15 min at 4°C, the supernatants were subjected to Western blot analysis as previously described (33) using Abs against COX-2 and iNOS (Santa Cruz Biotechnology). Glycogen content in the livers was assayed according a procedure described by Suzuki et al. (34). In brief, frozen liver tissues (50–100 mg) were hydrolyzed in 0.3 ml of 30% (w/v) KOH solution in a boiling water bath for 30 min. To facilitate digestion, the tubes were vigorously shaken by vortex every 10 min. After cooling to room temperature, 0.1 ml of 1 M Na_2SO_4 and 0.8 ml of ethanol were added; the samples were boiled again for 5 min to precipitate glycogen. Precipitated glycogen was pelleted by centrifugation at 20,000 × *g* for 10 min, and then washed twice with 70% ethanol. The pellet was first hydrolyzed in 0.5 ml of 4 N H_2SO_4 for 10 min at 100°C, and then the acidic solution was neutralized with 0.5 ml of 4 N NaOH. To determine the glucose concentration, 5 μl of the diluted sample was added to 0.2 ml of the glucose (HK) assay solution (Sigma-Aldrich). The glycogen concentration was determined by measuring the absorbance at 340 nm and glycogen content expressed as micromoles of glucosyl units per gram (wet weight).

Cytokine and nitrate measurement

The concentrations of TNF-α, IL-6, and IL-10 in serum were determined using ELISA kits (eBiosciences). Nitrate levels in the plasma were determined as previously described (23).

IL-10 neutralization

Mkp-1$^{-/-}$ mice received an i.v. injection of either 1 mg of monoclonal rat anti-mouse IL-10 Ab (JES5-2A5) or 1 mg of a monoclonal rat isotype control Ab (HRPN) (mAb Core of University of California, San Francisco) 60 min before i.v. challenge with live *E. coli* at 5 × 10^6 CFU/g of body weight. The blood and splenic bacterial loads were assessed 18 h postinfection. Separately, *Mkp-1*$^{-/-}$/*Il-10*$^{+/+}$ and *Mkp-1*$^{-/-}$/*Il-10*$^{-/-}$ double knockout mice were inoculated with 1 × 10^5 CFU/g and euthanized 18 h later to determine splenic bacterial load as described below.

Bacterial load determination

Mice were infected with *E. coli* and euthanized with i.p. pentobarbital 18 or 24 h postinfection. Blood and spleens were harvested aseptically. Each spleen was homogenized in 1 ml of sterile PBS. Spleen homogenates and blood were serially diluted in sterile PBS, plated onto separate Luria-Bertani agar plates, and the plates incubated for 18 h at 37°C. Colonies were counted separately for each sample. Spleen samples were normalized to organ weight, and blood samples were normalized to blood volume.

Statistical analyses

Survival differences between *Mkp-1*$^{-/-}$ and *Mkp-1*$^{+/+}$ mice and between *Mkp-1*$^{-/-}$/*Il-10*$^{+/+}$ and *Mkp-1*$^{-/-}$/*Il-10*$^{-/-}$ double knockout mice were analyzed by Kaplan-Meier analysis with log-rank test using the on-line statistics program (http://department.obg.cuhk.edu.hk/researchsupport/Survival.ASP) (Dr. Allan Chang, Department of Obstetrics and Gynaecology, Chinese University of Hong Kong). Differences in cytokine production, inflammatory markers, bacterial load, organ function markers, and lipid levels between groups were compared using SPSS statistics software. Data were log-transformed when deemed appropriate. A value of $p < 0.05$ was considered statistically significant for all analyses.

Results

The effect of Mkp-1 knockout on mortality and cytokine production following infection with live *E. coli* and CLP

To determine the function of Mkp-1 in the host response to live Gram-negative infection, we infected *Mkp-1*$^{+/+}$ and *Mkp-1*$^{-/-}$ mice i.v. with log-phase growth live *E. coli* at 2.5×10^7 CFU/g of body weight, a dose that was the LD_{50} for *Mkp-1*$^{+/+}$ mice by 72 h. There was significant mortality in the *Mkp-1*$^{+/+}$ group starting at 30 h postinfection, with a total mortality rate of 60%. In contrast, *Mkp-1*$^{-/-}$ mice began to die by 20 h postinfection and all *Mkp-1*$^{-/-}$ mice died during the observation period. Kaplan-Meier analysis revealed a significant difference in survival between the two groups (Fig. 1*A*).

To assess the impact of *Mkp-1* deficiency during subacute abdominal sepsis, we subjected *Mkp-1*$^{+/+}$ and *Mkp-1*$^{-/-}$ animals to CLP (Fig. 1*B*). As with live *E. coli*, onset of mortality in *Mkp-1*$^{-/-}$ mice was earlier than in *Mkp-1*$^{+/+}$ mice. The overall survival rate of *Mkp-1*$^{+/+}$ mice tended to be higher than that of *Mkp-1*$^{-/-}$ mice after CLP. However, this difference did not reach statistical significance ($p = 0.08$, $n = 15$/group).

To assess the role of Mkp-1 in cytokine production, *Mkp-1*$^{+/+}$ and *Mkp-1*$^{-/-}$ animals were infected with *E. coli* and sacrificed 18 h postinfection. Similar to previous reports of LPS-challenged mice, *Mkp-1*$^{-/-}$ mice produced markedly higher levels of both TNF-α and IL-6 compared with *Mkp-1*$^{+/+}$ animals. Interestingly, *Mkp-1*$^{-/-}$ mice also had increased IL-10 production (Fig. 1*C*).

Histopathological analyses

Since the lung is often compromised in cases of sepsis, we examined pulmonary histology in *Mkp-1*$^{+/+}$ and *Mkp-1*$^{-/-}$ mice 24 h after *E. coli* infection. Mice of both genotypes had comparable alveolar neutrophil infiltration (Fig. 2*A*) and this finding correlated with similar pulmonary MPO activity in *Mkp-1*$^{+/+}$ and *Mkp-1*$^{-/-}$ mice (Fig. 2*B*). In contrast *Mkp-1*$^{-/-}$ mice had a significantly higher lung/body weight ratio (Fig. 2*C*), indicating more severe pulmonary edema. Finally, the majority of *Mkp-1*$^{-/-}$ mice 24 h postinfection had dramatic pulmonary microvascular failure as evidenced by profound hemoconcentration in the pulmonary venules (Fig. 2*D*). Similar signs of hemoconcentration were also seen in *Mkp-1*$^{-/-}$ livers, kidneys, and thymuses (data not shown). In contrast, hemoconcentration was not seen in *Mkp-1*$^{+/+}$ mice (Fig. 2*D*).

Disruption of lipid and glycogen utilization in Mkp-1-deficient animals

Lipemic serum during sepsis has been documented both in animal models and human clinical cases, although the underlying mechanisms and clinical significance are not fully understood (19). Serum turbidity consistent with lipemia was consistently seen in *Mkp-1*$^{+/+}$ animals infected with 2.5×10^7 CFU/g *E. coli*, but not in infected *Mkp-1*$^{-/-}$ mice (Table I). Uninfected

Mkp-1$^{+/+}$ and *Mkp-1*$^{-/-}$ mice did not have lipemia (data not shown). The infection-associated lipemia in wild-type animals did not appear to be due to increased dietary fat intake, since infected mice of both strains were lethargic and did not appear to eat despite free access to food. To determine the role of Mkp-1 in infection-associated lipemia, sera were examined from *Mkp-1*$^{+/+}$ and *Mkp-1*$^{-/-}$ mice infected with a broad range of *E. coli* doses (Table I). Wild-type mice developed lipemia in a dose-dependent manner at doses higher than 1×10^6 CFU/g. In contrast, lipemia was absent in *Mkp-1*$^{-/-}$ mice within the tested range (Table I).

To understand the role of Mkp-1 in lipid metabolism during Gram-negative bacterial infection, we measured serum lipid levels in *Mkp-1*$^{+/+}$ and *Mkp-1*$^{-/-}$ mice 24 h after live *E. coli* infection. In uninfected animals, there were no significant differences between groups with regard to total plasma cholesterol or triglycerides. Following infection, blood cholesterol levels increased modestly in wild-type mice from 116.0 ± 9.5 to 153.7 ± 5.1 mg/dl (Fig. 3*A*) and triglyceride levels increased dramatically from 203.2 ± 42.7 to 1,218 ± 246 mg/dl (Fig. 3*B*). In contrast, *E. coli* infection did not significantly alter blood cholesterol or triglyceride levels in *Mkp-1*$^{-/-}$ mice. These results suggest that the *Mkp-1*$^{+/+}$ animals actively mobilized lipid stores in response to infection. The lack of triglyceride elevations above the uninfected baseline in *Mkp-1*$^{-/-}$ mice suggests a defect in mobilizing metabolic stores after infection.

In addition to lipid, glycogen is another key energy source that is rapidly mobilized during starvation and the stress response. We examined liver glycogen stores in *Mkp-1*$^{+/+}$ and *Mkp-1*$^{-/-}$ mice following infection (Fig. 3*C*). Uninfected mice of both genotypes had similar hepatic glycogen levels. After infection, hepatic glycogen in the *Mkp-1*$^{+/+}$ mice was substantially reduced, decreasing from 2.98 ± 0.99 to 0.20 ± 0.02 mg/g of liver tissue. In contrast, hepatic glycogen levels did not change significantly in *Mkp-1*$^{-/-}$ mice after infection. The defects in both triglyceride and glycogen metabolism are indicative of metabolic liver dysfunction in *E. coli*-infected *Mkp-1*$^{-/-}$ mice. These results also suggest that Mkp-1 is crucial for orchestrating a proper metabolic response during Gram-negative bacterial infection.

Organ function in Mkp-1-deficient mice

To understand the role of Mkp-1 in regulating organ function during *E. coli* infection, we measured organ biomarkers used clinically in human patients with sepsis (Table II). Although biomarker measurements were similar in the uninfected animals, several biomarkers were significantly different between *E. coli*-infected *Mkp-1*$^{+/+}$ and *Mkp-1*$^{-/-}$ mice. Aspartate aminotransferase and alanine aminotransferase are markers of liver injury. Aspartate aminotransferase activity in the infected *Mkp-1*$^{-/-}$ mice was significantly higher than in the infected *Mkp-1*$^{+/+}$ mice. Blood alanine aminotransferase activity in *Mkp-1*$^{-/-}$ mice tended to be higher than in the *Mkp-1*$^{+/+}$ mice, although the difference did not reach statistical significance. These results suggest that *Mkp-1*$^{-/-}$ mice suffered more severe liver injury than *Mkp-1*$^{+/+}$ mice after infection. Pancreatic amylase was reduced in infected *Mkp-1*$^{-/-}$ mice compared with uninfected whereas lipase enzyme activity was decreased in infected wild-type mice after infection. These enzymes are crucial for starch and lipid utilization, respectively. Moreover, creatinine kinase activity was significantly higher in the *Mkp-1*$^{-/-}$ mice than in the wild-type mice. This finding suggests that *Mkp-1*$^{-/-}$ mice suffered organ hypoperfusion secondary to reduced effective circulating volume, resulting in more severe myocardial and/or skeletal muscle injury. In addition, *Mkp-1*$^{-/-}$ mice had an elevated albumin/globulin ratio, indicating increased extravasation of plasma and small plasma proteins into the interstitial spaces. Surprisingly, *Mkp-1*$^{+/+}$ mice had significantly higher levels of urea nitrogen than did *Mkp-1*$^{-/-}$ mice, indicating either more severe dehydration or protein catabolism in wild-type mice (Table II). In summary, these findings support the histological evidence of capillary leakage, decreased circulating blood volume, and impaired organ perfusion in *Mkp-1*$^{-/-}$ mice.

Containment of infection and bacterial load after *E. coli* infection

Following microbial infection, the host employs a broad immune defense arsenal to contain and eliminate invading microorganisms, including phagocytosis by leukocytes and production of antimicrobial factors. Impaired innate immune responses can predispose the host to infection-associated illnesses, including septic shock. Since MAPKs are implicated in a myriad of cellular defense mechanisms, we examined the effects of *Mkp-1* knockout on bacterial burden. Splenic homogenates and blood samples were evaluated for bacterial CFU at 24 h postinoculation. *Mkp-1*$^{-/-}$ blood samples produced more bacterial colonies than samples from *Mkp-1*$^{+/+}$ mice (Fig. 4*A*). *Mkp-1*$^{-/-}$ splenic homogenates produced approximately 10-fold more bacterial colonies than wild-type samples. In summary, these data indicate that *Mkp-1*$^{-/-}$ mice have deficient bacterial clearance, which could contribute to the increased inflammatory activity and mortality seen after *E. coli* infection.

To determine potential mechanisms underlying the reduced antimicrobial activity in *Mkp-1*$^{-/-}$ mice, we examined several cytokines and antimicrobial factors. First, we evaluated the production of NO, a potent bactericidal substance critical for phagocyte killing of intracellular bacteria (35). Since NO is rapidly converted into nitrate, we measured blood nitrate levels as a surrogate for NO in infected *Mkp-1*$^{+/+}$ and *Mkp-1*$^{-/-}$ mice (Fig. 5*A*). Since *Mkp-1*$^{-/-}$ mice exhibited more severe hypotension in response to LPS and produced greater quantities of TNF-α and IL-6, we anticipated that these mice would produce greater levels of NO than wild-type mice. To our surprise, blood nitrate levels in *Mkp-1*$^{-/-}$ mice were actually significantly lower than those in the *Mkp-1*$^{+/+}$ mice. We next measured iNOS levels in *Mkp-1*$^{+/+}$ and *Mkp-1*$^{-/-}$ mice to see if altered enzyme levels were the cause of low nitrate levels in *Mkp-1*$^{-/-}$ mice (Fig. 5*B*). While pulmonary iNOS expression was not significantly different between infected *Mkp-1*$^{-/-}$ and *Mkp-1*$^{+/+}$ mice (Fig. 5*B*, *top*), iNOS expression in the livers of *Mkp-1*$^{-/-}$ mice was substantially lower than in *Mkp-1*$^{+/+}$ mice (Fig. 5*B*, *bottom*). The decreased iNOS expression is unlikely to be due to decreased sensitivity of these mice to inflammatory mediators such as cytokines. The expression of COX-2, another important mediator of inflammation, was substantially higher in both lung and liver in *E. coli*-infected *Mkp-1*$^{-/-}$ mice than in the infected *Mkp-1*$^{+/+}$ mice (Fig. 5*B*). Densitometry quantification of iNOS and COX-2 confirmed the decreases in iNOS expression and the increases in COX-2 expression in *Mkp-1*-deficient mice (Fig. 5*C*). These observations together with the lower NO levels in the blood of *Mkp-1*$^{-/-}$ mice (Fig. 5*A*) suggest that iNOS expression may be reduced in additional organs of *Mkp-1*$^{-/-}$ mice. These results also support the idea that *Mkp-1*$^{-/-}$ mice have diminished bactericidal activity, since insufficient NO could reduce bacterial killing efficiency.

To determine whether elevated IL-10 after infection is responsible for the diminished antimicrobial responses in *Mkp-1*$^{-/-}$ animals, knockout mice were treated with a neutralizing mAb specific for mouse IL-10 and then challenged with *E. coli*. A lower bacterial dose (5×10^6 CFU/g) was used since mice with markedly decreased IL-10 levels may have increased bacterial sensitivity. *Mkp-1*$^{-/-}$ mice treated with IL-10 neutralizing Ab exhibited significantly lower splenic bacterial load than mice administered control IgG1 Ab (Fig. 4*B*). Blood bacterial load was very low in both groups and not significantly different (data not shown). Finally, similar results were seen in *Mkp-1*$^{-/-}$/*Il-10*$^{-/-}$ double knockout mice infected with *E. coli* (1×10^5 CFU/g), with splenic bacterial load significantly lower in double knockout mice than in *Mkp-1*$^{-/-}$/*Il-10*$^{+/+}$ mice (Fig. 4*C*).

Antibiotic therapy, survival, and cytokine production

Timely antibiotic treatment is a current standard of care in human sepsis cases (32). We therefore examined the effect of antibiotic therapy in *E. coli*-infected *Mkp-1*$^{+/+}$ and *Mkp-1*$^{-/-}$ mice. Gentamicin treatment 3 h after infection with live *E. coli* resulted in dramatic differences in 72 h survival between the groups. Gentamicin therapy completely prevented

mortality in the *Mkp-1*$^{+/+}$ mice but had no impact on *Mkp-1*$^{-/-}$ survival, with all mice dying within 72 h (Fig. 6*A*). Although gentamicin treatment differentially affected the survival of the two groups of animals, it did not substantially alter the pattern of cytokine production in these mice (Fig. 6*B*).

Discussion

This is the first report to detail the responses of *Mkp-1*-deficient animals to live Gram-negative bacterial challenge, including mortality rate, inflammatory parameters, and clinical biomarkers of organ function. *Mkp-1*$^{-/-}$ animals had accelerated mortality after i.v. infection with live *E. coli* and had similarly decreased survival after CLP (Fig. 1). Increased mortality in *Mkp-1*$^{-/-}$ mice was accompanied by higher bacterial burdens (Fig. 4), elevated cytokine production (Fig. 1), higher COX-2 expression (Fig. 5), and yet attenuated NO production (Fig. 5). There were also marked differences in energy utilization between the two genotypes (Fig. 3 and Table I). Finally, we showed that the efficacy of bactericidal antimicrobial therapy depended on *Mkp-1* gene function (Fig. 6). Overall, these findings support a role for Mkp-1 in modulating the host response during Gram-negative infection, including regulating inflammation, metabolic resource distribution, and bacterial clearance.

The mortality rate and antimicrobial response of *Mkp-1*$^{-/-}$ mice in this study had both similarities and differences compared with related models. The increased mortality rate in *E. coli*-infected *Mkp-1*$^{-/-}$ mice was similar to the situation after LPS challenge (22,23). Surprisingly, Mkp-1 plays an important role in both host survival and bacterial clearance after *E. coli* infection, which is quite different from our previous study with *Staphylococcus aureus* (21). Mkp-1 is a crucial regulator of cytokine production during both bacterial infections (21). However, although Mkp-1 is required for *E. coli* clearance and host survival (Figs. 1 and 4), Mkp-1 does not appear to play an important role in determining the mortality rates and bacterial loads following *S. aureus* infection (21). Given these divergent findings, it was not surprising that *Mkp-1*$^{-/-}$ survival after CLP fell in between the two single bacterial models, with a clear trend toward an earlier and elevated mortality rate in *Mkp-1*$^{-/-}$ mice (Fig. 1*B*). CLP presents a polymicrobial challenge and more closely mimics postsurgical abdominal sepsis than single pathogen sepsis models.

Defects of Mkp-1-deficient mice in bactericidal mechanisms

Another key finding was the markedly attenuated bacterial clearance in *Mkp-1*$^{-/-}$ mice, evidenced by higher splenic and blood bacterial burdens. Since proinflammatory cytokines were higher in infected *Mkp-1*$^{-/-}$ mice (Fig. 1), these data suggest that *Mkp-1*$^{-/-}$ mice are not defective in the detection of *E. coli*. It is more likely that these mice have defects in bacterial capture or killing. Although the exact mechanism(s) underlying the defect(s) in *Mkp-1*$^{-/-}$ mice remains unclear, alterations in the innate immune response are most likely, since innate immunity is key to initial pathogen recognition, phagocytosis, and phagolysosomal killing (7). Altered production of several innate immune factors in *Mkp-1*$^{-/-}$ mice likely contributed to inhibited bacterial clearance.

First, levels of iNOS and nitrate (a reliable surrogate of NO) were lower in *Mkp-1*$^{-/-}$ mice (Fig. 5). NO is a potent bactericidal molecule (35) and decreased production in *Mkp-1*$^{-/-}$ mice may lead to attenuated bactericidal activity. Surprisingly, *Mkp-1*$^{-/-}$ mice exhibited elevated NO production after LPS challenge (21,23,36). These contrasting findings may be due to differences in the host immune responses to a purified bacterial component (LPS) vs intact bacteria. The combined responses to different *E. coli* components could produce a net reduction in iNOS expression in the *Mkp-1*$^{-/-}$ mouse. Alternatively, lower iNOS levels may be a compensatory host response to minimize blood pressure fluctuations. Thorough understanding

of the interplay of iNOS and Mkp-1 in anti-bacterial host responses will require additional studies.

A second factor that can potentially result in decreased bactericidal activity in *Mkp-1*$^{-/-}$ mice is the elevated IL-10 expression (Fig. 1). IL-10 is a pleotropic cytokine (37,38) that can potently inhibit production of reactive oxygen and nitrogen species, including NO, in macrophages (39). In peritonitis models, excess IL-10 compromises bacterial clearance (40), whereas IL-10 knockout potentiates *E. coli* elimination (41). IL-10 can inhibit pulmonary defense during sepsis (42) and prevent apoptosis of cells infected with pathogenic bacteria (37). In our study, *Mkp-1*$^{-/-}$ mice pre-treated with an IL-10 neutralizing Ab had significantly reduced splenic bacterial load. Similarly, infected *Mkp-1*$^{-/-}$/*Il-10*$^{-/-}$ double knockout mice also had lower splenic bacterial counts compared with *Mkp-1*$^{-/-}$ mice. Together, these experiments suggest an important role for IL-10 in depressing bacterial clearance in *Mkp-1*$^{-/-}$ mice.

Finally, excessive levels of COX-2 and the potential production of downstream mediators like prostaglandin E_2 may also be implicated in the compromised bactericidal activity of the *Mkp-1*$^{-/-}$ mice. It has been shown that prostaglandin E_2 inhibits macrophage production of reactive oxygen species and that knockout of either COX-2 or prostaglandin E_2 receptors enhance bacterial clearance in a pneumonia model (43). *E. coli*-infected *Mkp-1* knockout mice expressed higher COX-2 levels than did *Mkp-1*$^{+/+}$ mice (Fig. 5), suggesting that *Mkp-1*$^{-/-}$ mice might have elevated prostaglandin E_2 levels. However, we believe that elevated COX-2 expression is not likely a significant contributor to the compromised bactericidal activity in *Mkp-1*$^{-/-}$ mice, since treatment with the COX-2 inhibitor aspirin did not alter splenic or blood bacterial load in *Mkp-1*$^{-/-}$ mice (data not shown).

The function of Mkp-1 in the regulation of energy mobilization during sepsis

Systemic inflammation triggers release of energy stores to provide fuel for increased metabolic demands (17,44) and can lead to elevations in plasma lipids (lipemia of sepsis) (19). LPS can trigger inflammatory cytokines and sympathetic output from the autonomic nervous system to increase plasma triglyceride levels (45,46). Interestingly, new evidence shows that in addition to their role as an energy source, blood lipids may also function in the innate immune response. Infusion of chylomicrons, very low density lipoproteins, and triglyceride-rich lipids can sequester LPS, enhance LPS degradation in the liver, and dampen the host inflammatory response (47,48). In the present study, we found that *E. coli*-infected *Mkp-1*$^{-/-}$ mice failed to mobilize key lipid and carbohydrate energy stores (Fig. 3). Whereas infected *Mkp-1*$^{+/+}$ mice had markedly elevated serum triglycerides after infection, there was no change in *Mkp-1*$^{-/-}$ triglyceride levels. The absence of lipemia in infected *Mkp-1*$^{-/-}$ mice is unlikely to be an epiphenomenon of hyperinflammation, as both low and high inoculation doses failed to induce lipemia (Table I). In addition to altered lipid metabolism, *E. coli*-infected *Mkp-1*$^{+/+}$ mice demonstrated dramatic hepatic glycogen depletion, whereas liver glycogen in *Mkp-1*$^{-/-}$ mice was unaltered. This finding was unexpected, as blood glucose levels in infected *Mkp-1*$^{+/+}$ and *Mkp-1*$^{-/-}$ mice were similar (Table II) and severe inflammation is known to perturb glucose homeostasis (49–51). Although the exact mechanism underlying defective lipid and glycogen mobilization in *Mkp-1*$^{-/-}$ mice remains unclear, these defects may be related to metabolic abnormalities previously reported by another laboratory. Wu et al. (52) have demonstrated that *Mkp-1* deletion accelerates energy catabolism, resulting in leaner body mass, decreased adiposity, and accelerated hepatic lipid metabolism. Given these reported differences in body mass and adipose depots, it was surprising that blood baseline triglyceride and glycogen levels were comparable in *Mkp-1*$^{+/+}$ and *Mkp-1*$^{-/-}$ mice in the absence of infection (Fig. 3). These findings indicate that Mkp-1 may have divergent roles in maintaining blood and tissue energy stores. In other words, while Mkp-1 plays a significant role in maintaining the normal metabolism in the absence of infection, it becomes critical in mobilizing energy resources when

the host must combat infectious pathogens. Since Mkp-1 is a negative regulator of MAPKs, the protein most likely serves as an upstream regulator of energy catabolism rather than having direct interactions with individual lipolysis and glycogenolysis pathways.

The importance of Mkp-1 in determining outcome after antibiotic therapy

Although gentamicin therapy was protective for 100% of *Mkp-1*$^{+/+}$ mice, it did not decrease mortality in *Mkp-1*$^{-/-}$ mice (Fig. 6). This phenomenon may be due to our use of a bactericidal antibiotic, which lyses bacteria and may cause the release of large quantities of endotoxin, thus mimicking an LPS challenge model. In such a case, high rates of mortality in *Mkp-1*$^{-/-}$ mice are not surprising, since these mice are exquisitely sensitive to LPS challenge (22,23). The absence of any protective response after antibiotic treatment suggests that excessive cytokine production in high-dose infected *Mkp-1*$^{-/-}$ mice is severe enough to mitigate any benefit from bacterial killing. In contrast, the potent reduction in mortality of *Mkp-1*$^{+/+}$ mice after antibiotic treatment indicates that decreased bacterial burden promotes survival, so long as the animals are not hypersensitive to endotoxin. Ultimately, bacterio-static antibiotics such as protein synthesis inhibitors may decrease bacterial load with limited endotoxin release and potentially increase *Mkp-1*$^{-/-}$ mouse survival.

Although MKP-1 activity in septic human patients has not directly been studied, several findings indicate that the protein will be a clinically relevant factor. First, MKPs are highly conserved across species and appear to function similarly in humans. Second, reduced MKP-1 expression in the lung can be seen clinically, as has been shown for immune cells isolated from human asthma patients (53,54). Finally, sepsis and multiple organ dysfunction syndrome in humans are systemic inflammatory diseases mechanistically similar to the animal models reported in this study. If MKP-1 in humans shows similar potent anti-inflammatory activity, supports bactericidal activity of the immune system, and facilitates resource utilization, modulation of MKP-1 will be a valuable therapeutic target for patients suffering from septic shock and multiple organ dysfunction syndrome.

Acknowledgments

We are grateful to Bristol-Myers Squibb Pharmaceutical Research Institute for providing Mkp-1 knockout mice. We thank Dr. Yi Jin for assistance measuring serum nitrates. We also gratefully acknowledge Sylvia Tozbikian, Joshua Kuhlman, and Nan Zhang for technical support. We thank Drs. James Cooper and Laura Goodchild for vivarium expertise and Dr. Richard Ye for thoughtful insight and discussion.

References

1. Angus DC, Linde-Zwirble WT, Lidicker J, Clermont G, Carcillo J, Pinsky MR. Epidemiology of severe sepsis in the United States: analysis of incidence, outcome, and associated costs of care. Crit Care Med 2001;29:1303–1310. [PubMed: 11445675]
2. Angus DC, Wax RS. Epidemiology of sepsis: an update. Crit Care Med 2001;29:S109–S116. [PubMed: 11445744]
3. Hotchkiss RS I, Karl E. The pathophysiology and treatment of sepsis. N Engl J Med 2003;348:138–150. [PubMed: 12519925]
4. Beutler B. TNF, immunity and inflammatory disease: lessons of the past decade. J Investig Med 1995;43:227–235.
5. Beutler B, Bazzoni F. TNF, apoptosis and autoimmunity: a common thread? Blood Cells Mol Dis 1998;24:216–230. [PubMed: 9645922]
6. O'Shea JJ, Ma A, Lipsky P. Cytokines and autoimmunity. Nat Rev Immunol 2002;2:37–45. [PubMed: 11905836]
7. Janeway, J.; Charles, A.; Travers, P.; Walport, M.; Schlomchik, MJ. Immunobiology: the immune system in health and disease. Garland Science; New York: 2005.

8. Cohen J. The immunopathogenesis of sepsis. Nature 2002;420:885–891. [PubMed: 12490963]
9. Fisher CJ Jr, Agosti JM, Opal SM, Lowry SF, Balk RA, Sadoff JC, Abraham E, Schein RM, Benjamin E. Treatment of septic shock with the tumor necrosis factor receptor:Fc fusion protein. The Soluble TNF Receptor Sepsis Study Group. N Engl J Med 1996;334:1697–1702. [PubMed: 8637514]
10. Parrillo JE. Pathogenetic mechanisms of septic shock. N Engl J Med 1993;328:1471–1477. [PubMed: 8479467]
11. Spiller S, Elson G, Ferstl R, Dreher S, Mueller T, Freudenberg M, Daubeuf B, Wagner H, Kirschning CJ. TLR4-induced IFN-γ production increases TLR2 sensitivity and drives Gram-negative sepsis in mice. J Exp Med 2008;205:1747–1754. [PubMed: 18644971]
12. Liu Y, Shepherd EG, Nelin LD. MAPK phosphatases—regulating the immune response. Nat Rev Immunol 2007;7:202–212. [PubMed: 17318231]
13. Wu JJ, Bennett AM. Essential role for mitogen-activated protein (MAP) kinase phosphatase-1 in stress-responsive MAP kinase and cell survival signaling. J Biol Chem 2005;280:16461–16466. [PubMed: 15722358]
14. Beutler B. Tlr4: central component of the sole mammalian LPS sensor. Curr Opin Immunol 2000;12:20–26. [PubMed: 10679411]
15. Klebanoff SJ. Myeloperoxidase: friend and foe. J Leukocyte Biol 2005;77:598–625. [PubMed: 15689384]
16. Serbina NV, Salazar-Mather TP, Biron CA, Kuziel WA, Pamer EG. TNF/iNOS-producing dendritic cells mediate innate immune defense against bacterial infection. Immunity 2003;19:59–70. [PubMed: 12871639]
17. Plank LD, Connolly AB, Hill GL. Sequential changes in the metabolic response in severely septic patients during the first 23 days after the onset of peritonitis. Ann Surg 1998;228:146–158. [PubMed: 9712558]
18. Trager K, DeBacker D, Radermacher P. Metabolic alterations in sepsis and vasoactive drug-related metabolic effects. Curr Opin Crit Care 2003;9:271–278. [PubMed: 12883281]
19. Harris HW, Gosnell JE, Kumwenda ZL. The lipemia of sepsis: triglyceride-rich lipoproteins as agents of innate immunity. J Endotoxin Res 2000;6:421–430. [PubMed: 11521066]
20. Kattan OM, Kasravi FB, Elford EL, Schell MT, Harris HW. Apolipoprotein E-mediated immune regulation in sepsis. J Immunol 2008;181:1399–1408. [PubMed: 18606694]
21. Wang X, Meng X, Kuhlman JR, Nelin LD, Nicol KK, English BK, Liu Y. Knockout of Mkp-1 enhances the host inflammatory responses to Gram-positive bacteria. J Immunol 2007;178:5312–5320. [PubMed: 17404316]
22. Zhao Q, Shepherd EG, Manson ME, Nelin LD, Sorokin A, Liu Y. The role of mitogen-activated protein kinase phosphatase-1 in the response of alveolar macrophages to lipopolysaccharide: attenuation of proinflammatory cytokine biosynthesis via feedback control of p38. J Biol Chem 2005;280:8101–8108. [PubMed: 15590669]
23. Zhao Q, Wang X, Nelin LD, Yao Y, Matta R, Manson ME, Baliga RS, Meng X, Smith CV, Bauer JA, et al. MAP kinase phosphatase 1 controls innate immune responses and suppresses endotoxic shock. J Exp Med 2006;203:131–140. [PubMed: 16380513]
24. Chi H, Barry SP, Roth RJ, Wu JJ, Jones EA, Bennett AM, Flavell RA. Dynamic regulation of pro- and anti-inflammatory cytokines by MAPK phosphatase 1 (MKP-1) in innate immune responses. Proc Natl Acad Sci USA 2006;103:2274–2279. [PubMed: 16461893]
25. Hammer M, Mages J, Dietrich H, Servatius A, Howells N, Cato AC, Lang R. Dual specificity phosphatase 1 (DUSP1) regulates a subset of LPS-induced genes and protects mice from lethal endotoxin shock. J Exp Med 2006;203:15–20. [PubMed: 16380512]
26. Salojin KV I, Owusu B, Millerchip KA, Potter M, Platt KA, Oravecz T. Essential role of MAPK phosphatase-1 in the negative control of innate immune responses. J Immunol 2006;176:1899–1907. [PubMed: 16424221]
27. Dorfman K, Carrasco D, Gruda M, Ryan C, Lira SA, Bravo R. Disruption of the erp/mkp-1 gene does not affect mouse development: normal MAP kinase activity in ERP/MKP-1-deficient fibroblasts. Oncogene 1996;13:925–931. [PubMed: 8806681]
28. Kuhn R, Lohler J, Rennick D, Rajewsky K, Muller W. Interleukin-10-deficient mice develop chronic enterocolitis. Cell 1993;75:263–274. [PubMed: 8402911]

29. Guo L, Song Z, Li M, Wu Q, Wang D, Feng H, Bernard P, Daugherty A, Huang B, Li XA. Scavenger receptor BI protects against septic death through its role in modulating inflammatory response. J Biol Chem 2009;284:19826–19834. [PubMed: 19491399]
30. Dellinger RP, Levy MM, Carlet JM, Bion J, Parker MM, Jaeschke R, Reinhart K, Angus DC, Brun-Buisson C, Beale R, et al. Surviving Sepsis Campaign: international guidelines for management of severe sepsis and septic shock: 2008. Crit Care Med 2008;36:296–327. [PubMed: 18158437]
31. Rivers E, Nguyen B, Havstad S, Ressler J, Muzzin A, Knoblich B, Peterson E, Tomlanovich M. Early goal-directed therapy in the treatment of severe sepsis and septic shock. N Engl J Med 2001;345:1368–1377. [PubMed: 11794169]
32. Brierley J, Carcillo JA, Choong K, Cornell T, Decaen A, Deymann A, Doctor A, Davis A, Duff J, Dugas MA, et al. Clinical practice parameters for hemodynamic support of pediatric and neonatal septic shock: 2007 update from the American College of Critical Care Medicine. Crit Care Med 2009;37:666–688. [PubMed: 19325359]
33. Chen P, Li J, Barnes J, Kokkonen GC, Lee JC, Liu Y. Restraint of proinflammatory cytokine biosynthesis by mitogen-activated protein kinase phosphatase-1 in lipopolysaccharide-stimulated macrophages. J Immunol 2002;169:6408–6416. [PubMed: 12444149]
34. Suzuki Y, Lanner C, Kim JH, Vilardo PG, Zhang H, Yang J, Cooper LD, Steele M, Kennedy A, Bock CB, et al. Insulin control of glycogen metabolism in knockout mice lacking the muscle-specific protein phosphatase PP1G/RGL. Mol Cell Biol 2001;21:2683–2694. [PubMed: 11283248]
35. Bogdan C. Nitric oxide and the immune response. Nat Immunol 2001;2:907–916. [PubMed: 11577346]
36. Nelin LD, Wang X, Zhao Q, Chicoine LG, Young TL, Hatch DM, English BK, Liu Y. MKP-1 switches arginine metabolism from nitric oxide synthase to arginase following endotoxin challenge. Am J Physiol Cell Physiol 2007;293:C632–C640. [PubMed: 17442735]
37. Couper KN, Blount DG, Riley EM. IL-10: the master regulator of immunity to infection. J Immunol 2008;180:5771–5777. [PubMed: 18424693]
38. Redpath S, Ghazal P, Gascoigne NR. Hijacking and exploitation of IL-10 by intracellular pathogens. Trends Microbiol 2001;9:86–92. [PubMed: 11173248]
39. Bogdan C, Vodovotz Y, Nathan C. Macrophage deactivation by interleukin 10. J Exp Med 1991;174:1549–1555. [PubMed: 1744584]
40. Reddy RC, Chen GH, Newstead MW, Moore T, Zeng X, Tateda K, Standiford TJ. Alveolar macrophage deactivation in murine septic peritonitis: role of interleukin 10. Infect Immun 2001;69:1394–1401. [PubMed: 11179304]
41. Sewnath ME, Olszyna DP, Birjmohun R, ten Kate FJ, Gouma DJ, van Der Poll T. IL-10-deficient mice demonstrate multiple organ failure and increased mortality during *Escherichia coli* peritonitis despite an accelerated bacterial clearance. J Immunol 2001;166:6323–6331. [PubMed: 11342656]
42. Steinhauser ML, Hogaboam CM, Kunkel SL, Lukacs NW, Strieter RM, Standiford TJ. IL-10 is a major mediator of sepsis-induced impairment in lung antibacterial host defense. J Immunol 1999;162:392–399. [PubMed: 9886412]
43. Sadikot RT, Zeng H, Azim AC, Joo M, Dey SK, Breyer RM, Peebles RS, Blackwell TS, Christman JW. Bacterial clearance of *Pseudomonas aeruginosa* is enhanced by the inhibition of COX-2. Eur J Immunol 2007;37:1001–1009. [PubMed: 17330822]
44. Gabay C, Kushner I. Acute-phase proteins and other systemic responses to inflammation. N Engl J Med 1999;340:448–454. [PubMed: 9971870]
45. Feingold KR, Serio MK, Adi S, Moser AH, Grunfeld C. Tumor necrosis factor stimulates hepatic lipid synthesis and secretion. Endocrinology 1989;124:2336–2342. [PubMed: 2707158]
46. Nonogaki K, Moser AH, Feingold KR, Grunfeld C. Alpha-adrenergic receptors mediate the hypertriglyceridemia induced by endotoxin, but not tumor necrosis factor, in rats. Endocrinology 1994;135:2644–2650. [PubMed: 7988454]
47. Eichbaum EB, Harris HW, Kane JP, Rapp JH. Chylomicrons can inhibit endotoxin activity in vitro. J Surg Res 1991;51:413–416. [PubMed: 1758174]
48. Harris HW, Grunfeld C, Feingold KR, Rapp JH. Human very low density lipoproteins and chylomicrons can protect against endotoxin-induced death in mice. J Clin Invest 1990;86:696–702. [PubMed: 2394827]

49. Ali NA, O'Brien JM Jr, Dungan K, Phillips G, Marsh CB, Lemeshow S, Connors AF Jr, Preiser JC. Glucose variability and mortality in patients with sepsis. Crit Care Med 2008;36:2316–2321. [PubMed: 18596625]
50. Hirshberg E, Larsen G, Van Duker H. Alterations in glucose homeostasis in the pediatric intensive care unit: hyperglycemia and glucose variability are associated with increased mortality and morbidity. Pediatr Crit Care Med 2008;9:361–366. [PubMed: 18496414]
51. Van den Berghe G, Wilmer A, Hermans G, Meersseman W, Wouters PJ, Milants I, Van Wijngaerden E, Bobbaers H, Bouillon R. Intensive insulin therapy in the medical ICU. N Engl J Med 2006;354:449–461. [PubMed: 16452557]
52. Wu JJ, Roth RJ, Anderson EJ, Hong EG, Lee MK, Choi CS, Neufer PD, Shulman GI, Kim JK, Bennett AM. Mice lacking MAP kinase phosphatase-1 have enhanced MAP kinase activity and resistance to diet-induced obesity. Cell Metab 2006;4:61–73. [PubMed: 16814733]
53. Bhavsar P, Hew M, Khorasani N, Torrego A, Barnes PJ, Adcock I, Chung KF. Relative corticosteroid insensitivity of alveolar macrophages in severe asthma compared with non-severe asthma. Thorax 2008;63:784–790. [PubMed: 18492738]
54. Sutherland ER, Goleva E, Strand M, Beuther DA, Leung DY. Body mass and glucocorticoid response in asthma. Am J Respir Crit Care Med 2008;178:682–687. [PubMed: 18635892]

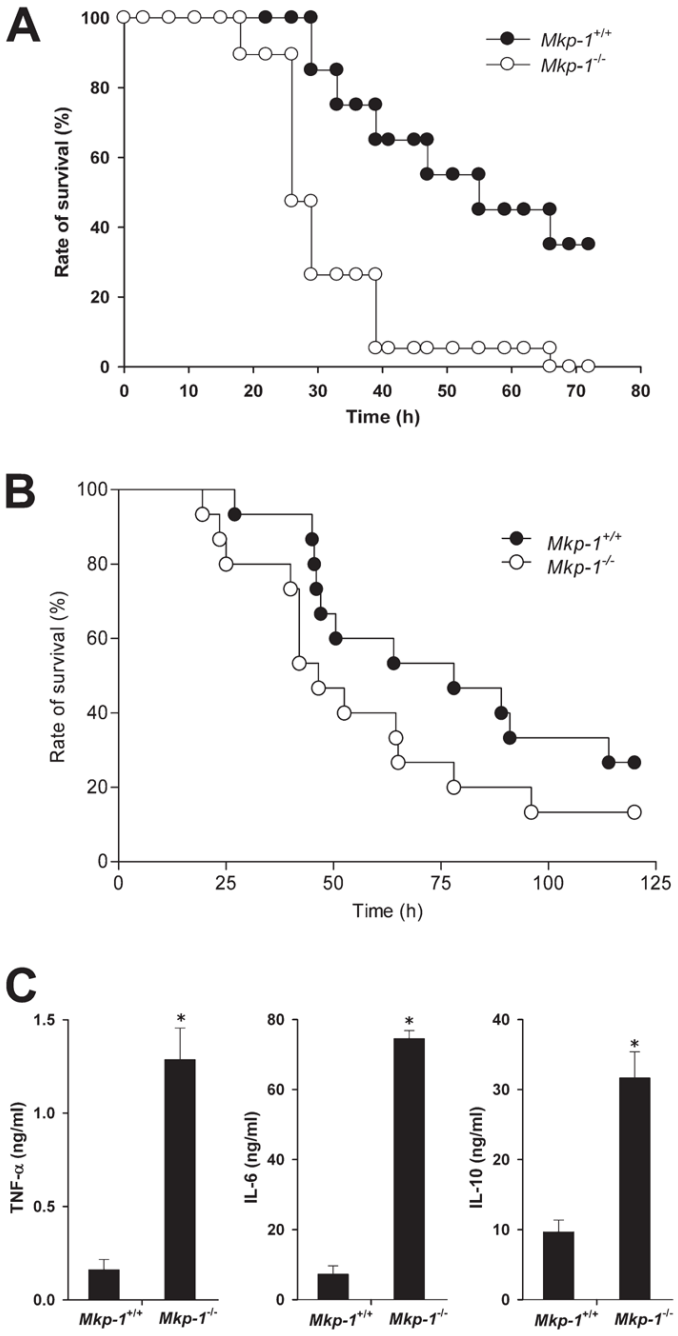

FIGURE 1.

Survival and cytokine production following infection with live *E. coli* and following CLP. *A*, Survival curves of *Mkp-1*$^{-/-}$ and *Mkp-1*$^{+/+}$ mice after i.v. infection of live *E. coli*. Mkp-1$^{-/-}$ and *Mkp-1*$^{+/+}$ mice were infected i.v. with live *E. coli* at a dose of 2.5×10^7 CFU/g of body weight. Mice were monitored continuously for 3 days. Kaplan-Meier analysis demonstrates significantly accelerated mortality in *Mkp-1*$^{-/-}$ mice ($n = 19$) compared with *Mkp-1*$^{+/+}$ mice ($n = 20$), $p = 0.001$. *B*, Survival curves of *Mkp-1*$^{+/+}$ and *Mkp-1*$^{-/-}$ mice after cecal ligation and puncture. *Mkp-1*$^{-/-}$ mice ($n = 15$) trended toward increased sensitivity to *E. coli* infection and exhibit earlier and higher mortality than *Mkp-1*$^{+/+}$ mice ($n = 15$), $p = 0.08$. *C*, Serum cytokine levels in *Mkp-1*$^{+/+}$ and *Mkp-1*$^{-/-}$ mice after *E. coli* infection. Mice were euthanized 18 h

following *E. coli* infection (2.5×10^7 CFU/g). Blood was collected by cardiac puncture, and cytokines measured by ELISA. *, $p < 0.05$, compared with *Mkp-1*$^{+/+}$ mice. $n = 8$.

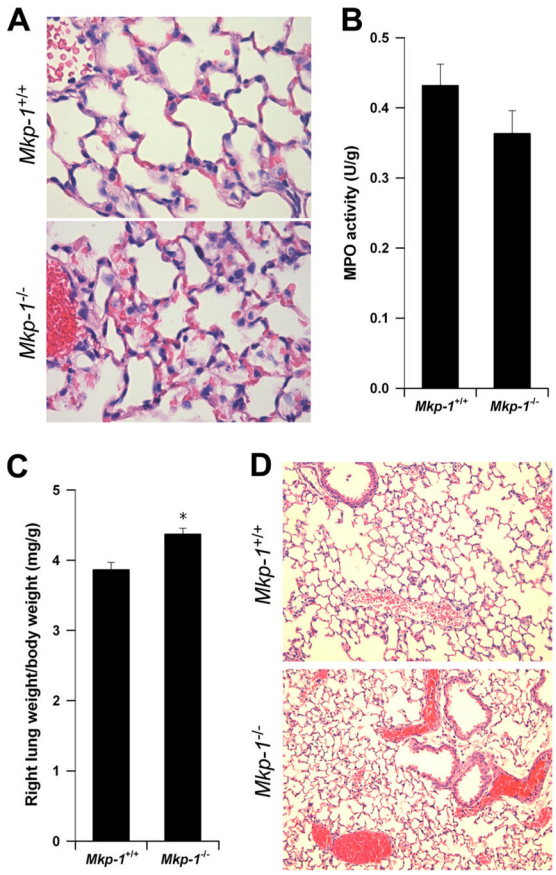

FIGURE 2.

Pulmonary edema and hemoconcentration in *Mkp-1*$^{-/-}$ mice. *Mkp-1*$^{-/-}$ and *Mkp-1*$^{+/+}$ mice were infected i.v. with live *E. coli* at a dose of 2.5×10^7 CFU/g of body weight and euthanized 24 h later. The left lungs were inflated, fixed, and stained with H&E. *A*, Histology of *Mkp-1*$^{+/+}$ and *Mkp-1*$^{-/-}$ mice demonstrated neutrophil infiltrates in the lung following infection. *B*, MPO activity in the lungs. The right lungs were harvested, weighed, and MPO activity was measured. The values were normalized to the tissue weights. Results represent the means ± SE of five independent animals. *C*, More severe pulmonary edema in the *Mkp-1*$^{-/-}$ mice than in the *Mkp-1*$^{+/+}$ mice after *E. coli* infection. Data represent the relative right lung weights in *Mkp-1*$^{+/+}$ and *Mkp-1*$^{-/-}$ mice after *E. coli* infection. Values are the right lung weight/total body weight, and are expressed as means ± SE of five independent mice. *, $p < 0.05$, compared with wild-type mice. *D*, Hemoconcentration in *Mkp-1*$^{-/-}$ but not in *Mkp-1*$^{+/+}$ mice. Results shown in *A* and *D* were from representative experiments.

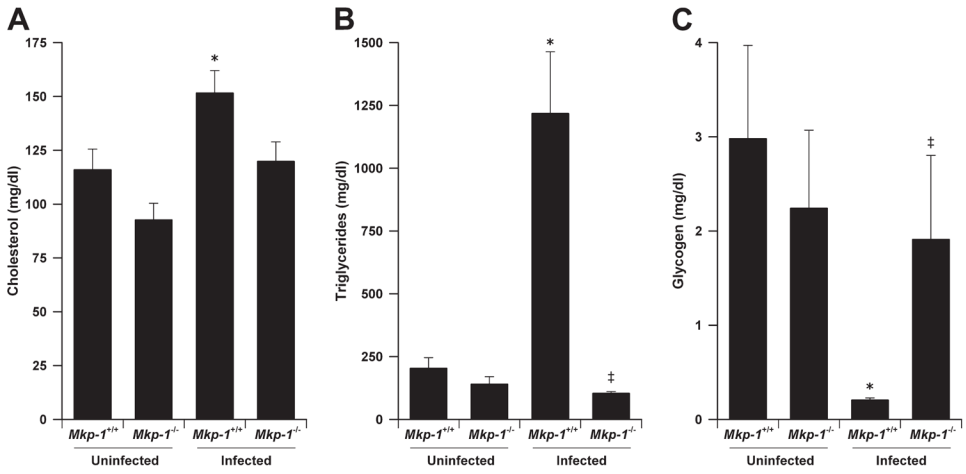

FIGURE 3.

Regulation of lipid and glucose metabolism by Mkp-1. *Mkp-1*$^{-/-}$ and *Mkp-1*$^{+/+}$ mice were infected i.v. with live *E. coli* at a dose of 2.5×10^7 CFU/g of body weight. Animals were euthanized 24 h later to harvest blood and livers. Uninfected mice were used as controls. The serum was analyzed for lipid concentrations. The livers were processed to measure glycogen concentrations. *A*, Total cholesterol levels in uninfected and *E. coli*-infected mice. *B*, Total triglycerides in uninfected and infected mice. *C*, Hepatic glycogen levels in uninfected and infected mice. Values in the graphs represent means ± SE from at least five independent mice. *, Different from uninfected *Mkp-1*$^{+/+}$ mice ($p < 0.05$). ‡, Different from *E. coli*-infected *Mkp-1*$^{+/+}$ mice ($p < 0.05$).

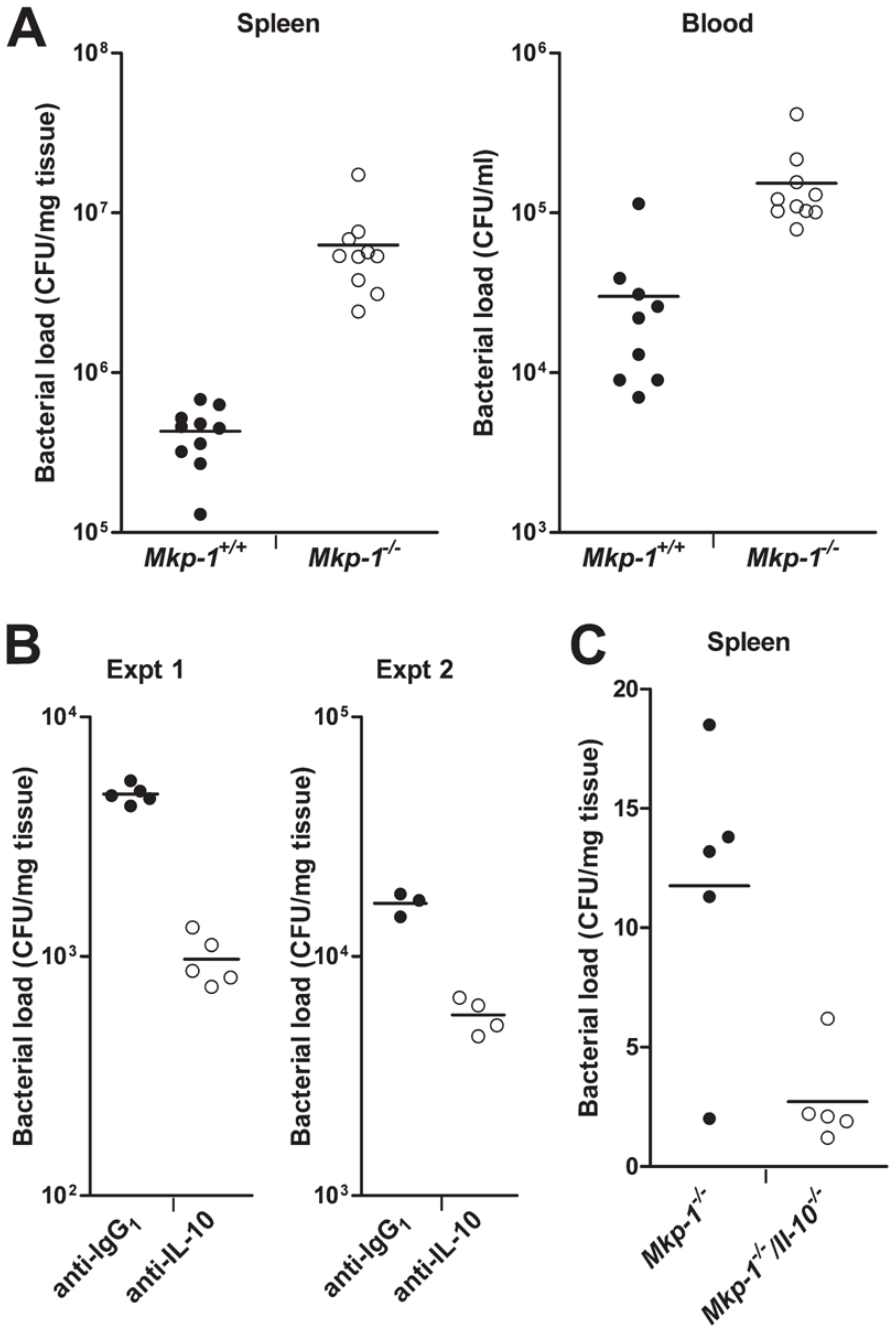

FIGURE 4.

Defect of *Mkp-1*$^{-/-}$ mice in the containment of bacteria. *A*, Lower bacterial load in *Mkp-1*$^{+/+}$ mice than in *Mkp-1*$^{-/-}$ mice after *E. coli* infection. Mice were infected i.v. with live *E. coli* at a dose of 2.5×10^7 CFU/g of body weight, and euthanized 24 h later. Blood and spleens were excised aseptically. Blood and spleen homogenates were cultured on Luria-Bertani agar plates. Colony numbers were normalized to volume (for blood) and tissue weight (for spleens). Data represent the bacterial load in spleen and blood. $p < 0.05$, comparing *Mkp-1*$^{+/+}$ with *Mkp-1*$^{-/-}$, $n = 10$. *B*, Effect of IL-10 neutralization on splenic bacterial load in *Mkp-1*$^{-/-}$ mice. *Mkp-1*$^{-/-}$ mice were administered either 1 mg of α-IL-10 mAb or 1 mg of an isotype control rat mAb i.v.. Animals were then infected with live *E. coli* 60 min later at a dose of 5×10^6

CFU/g of body weight. Mice were euthanized 18 h later to evaluate bacterial burden. Values in the graphs represent two separate experiments. IL-10 neutralization resulted in less splenic bacterial load compared with untreated *Mkp-1*$^{-/-}$ mice ($p < 0.05$). *C*, Bacterial load in *Mkp-1*$^{-/-}$ and *Mkp-1*$^{-/-}$/*Il-10*$^{-/-}$ double knockout mice. Animals were infected with live *E. coli* at a dose of 1×10^5 CFU/g. Mice were euthanized at 18 h to evaluate bacterial load. *Mkp-1*$^{-/-}$/*Il-10*$^{-/-}$ mice exhibited lower splenic bacterial load than *Mkp-1*$^{-/-}$ mice ($p < 0.05$). In all experiments, horizontal line represents mean value of CFU.

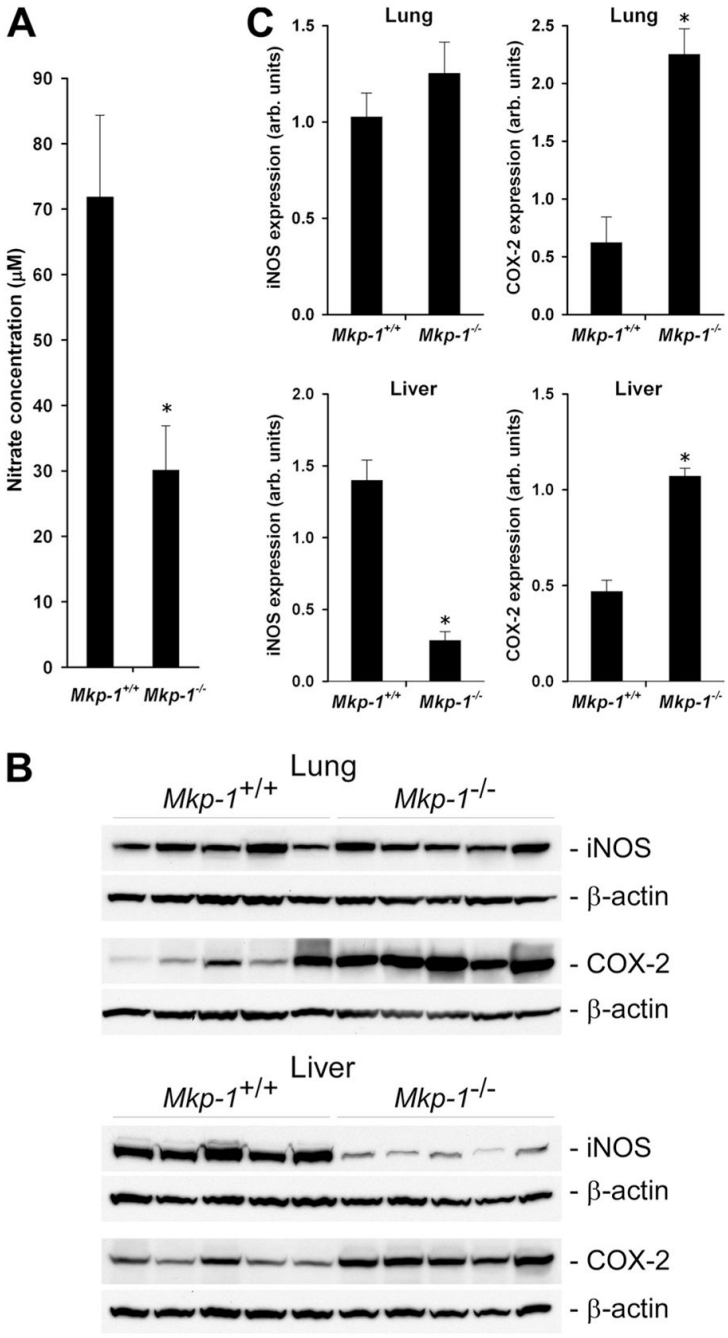

FIGURE 5.

Nitrate production and expression of iNOS and COX-2 in organs after *E. coli* infection. *Mkp-1*$^{-/-}$ and *Mkp-1*$^{+/+}$ mice were infected i.v. with live *E. coli* at a dose of 2.5×10^7 CFU/g of body weight. Animals were euthanized 24 h later to harvest blood and organs. *A*, The concentration of nitrates in the plasma. Values represents the means ± SE of eight independent animals. *B*, Western blot analyses of iNOS and COX-2 expression in the lungs and livers. Tissues were homogenated to extract protein, and equal amounts of protein were analyzed by Western blot analyses using Abs specific for iNOS or COX-2. The membranes were stripped and re-blotted with *β*-actin Ab to control for comparable loading. *C*, Quantitation of iNOS and COX-2 expression in the lungs and livers. The intensities of the Western blot protein bands of

interest were measured by densitometry. Values of iNOS or COX-2 were divided by the values of β-actin and presented in the graph as means ± SE from five different animals. *, $p < 0.05$, compared with *Mkp-1*$^{+/+}$ group.

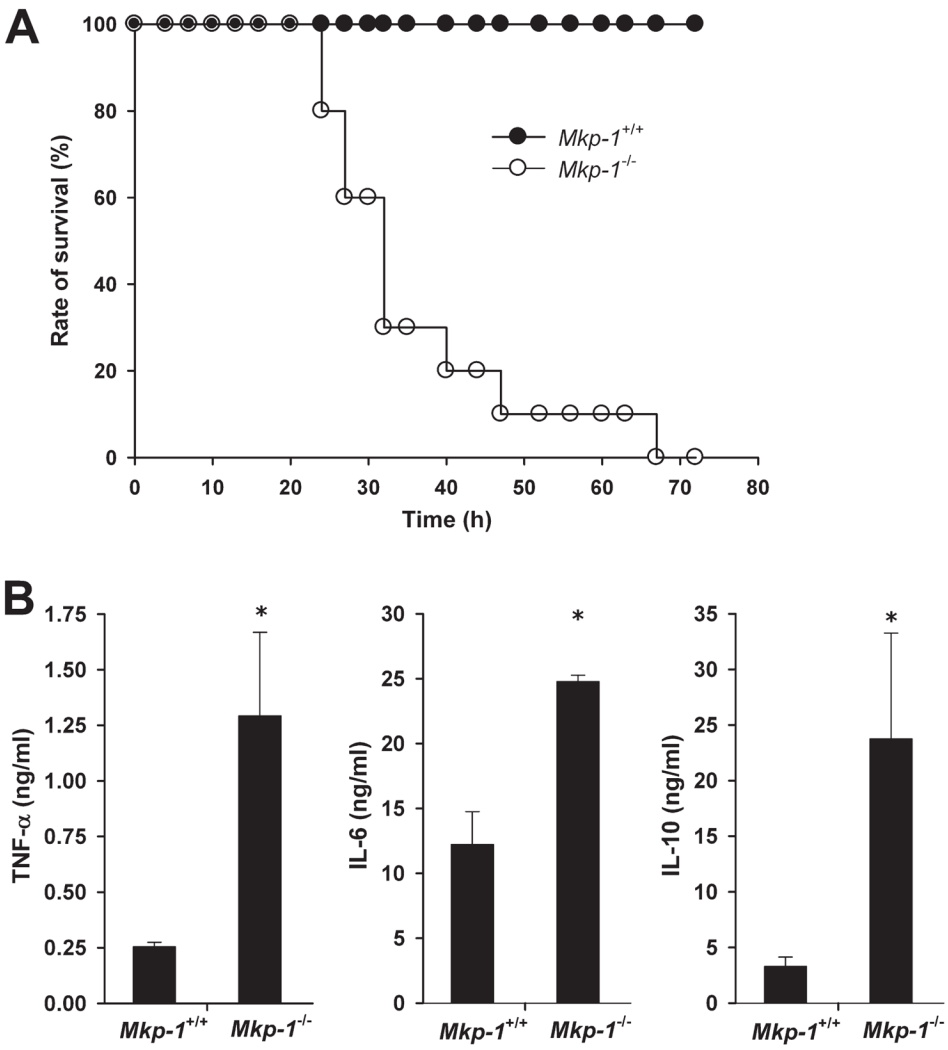

FIGURE 6.

Prevention of mortality in *E. coli*-infected *Mkp-1*$^{+/+}$ mice but not in infected *Mkp-1*$^{-/-}$ mice by gentamicin. *Mkp-1*$^{+/+}$ and *Mkp-1*$^{-/-}$ mice were infected i.v. with live *E. coli* at a dose of 2.5×10^7 CFU/g of body weight. Three hours later, mice were treated with 25 μg of gentamicin dissolved in 1 ml of PBS. *A*, Survival curves of gentamicin-treated *Mkp-1*$^{+/+}$ and *Mkp-1*$^{-/-}$ mice. Survival in the two strains of mice were compared by Kaplan-Meier analysis and found to be significantly different ($p < 0.0001$). *B*, Cytokine production in *E. coli*-infected mice after gentamicin treatment. Mice were infected with *E. coli* and treated with gentamicin. These animals were euthanized 18 h after the initial infection, and ELISA used to measured cytokines in the blood. Values in the graphs represent the means ± SE from five to eight mice. *, different from *Mkp-1*$^{+/+}$ mice ($p < 0.05$).

Table I

Development of lipemia in mice after *E. coli* infection[a]

Dose of Infection (CFU/g)	Portion of Lipemic Mice (lipemic/total)	
	Mkp-1$^{+/+}$	*Mkp-1*$^{-/-}$
2.5×10^7	14/20	0/30
1×10^7	12/19	0/20
9×10^6	8/8	0/8
1×10^6	0/5	0/5
5×10^5	0/5	0/5

[a]Mice were infected i.v. with *E. coli* and euthanized 24 h later. Blood was collected by cardiac puncture. Lipemia was defined as the appearance of cloudy serum and was confirmed by lipid panel analysis.

Table II

Metabolic analyses of *Mkp-1*$^{+/+}$ and *Mkp-1*$^{-/-}$ mice[a]

	Uninfected		Infected	
Biomarker	***Mkp-1*$^{+/+}$**	***Mkp-1*$^{-/-}$**	***Mkp-1*$^{+/+}$**	***Mkp-1*$^{-/-}$**
ALT (U/L)	36.4 ± 4.5	24.4 ± 2.4	182.3 ± 22.2*	459.4 ± 146†
AST (U/L)	391.8 ± 71.8	202.6 ± 32.8	712.6 ± 133	1,497 ± 237†,‡
Amylase (U/L)	2717 ± 164	2829 ± 273	2,987 ± 356	1,695 ± 115†,‡
Glucose (mg/dl)	256 ± 7.7	285 ± 0.11	70.1 ± 6.8*	100.3 ± 13.9†
Lipase (U/L)	281 ± 9	239 ± 21	159 ± 15	300 ± 40*
CK (U/L)	850 ± 164	583 ± 96	3,069 ± 372*	6,676 ± 1,053†,‡
Urea nitrogen (mg/dl)	29.4 ± 2.2	25.6 ± 1.1	101.4 ± 4.6*	76.3 ± 2.8†,‡
Creatinine (mg/dl)	0.2 ± 0.0	0.2 ± 0.0	0.53 ± 0.08	0.6 ± 0.0
Anion gap (mEq/l)	42.6 ± 0.87	41.4 ± 0.92	31.4 ± 1.4*	27.1 ± 2.6†
Total protein (g/dl)	4.9 ± 0.13	5.06 ± 0.05	4.6 ± 0.12	4.7 ± 0.53
Albumin (g/dl)	3.46 ± 0.06	3.56 ± 0.04	3.02 ± 0.1*	3.69 ± 0.46
Albumin/globulin ratio	2.44 ± 0.11	2.4 ± 0.11	1.94 ± 0.09*	4.21 ± 0.85‡

[a]Infected mice were injected i.v. with 2.5×10^7 CFU/g of *E. coli* and euthanized 24 h later. Blood was collected by cardiac puncture. Serum was analyzed for complete biomarkers. Data are presented as mean ± SE ($n = 7$).

$^{*}p < 0.05$ vs uninfected *Mkp-1*$^{+/+}$ mice;

$^{\dagger}p < 0.05$ vs uninfected *Mkp-1*$^{-/-}$ mice;

$^{\ddagger}p < 0.05$ vs infected *Mkp-1*$^{+/+}$ mice.